DMD Fast Forward. Published on April 14, 2017 as DOI: 10.1124/dmd.116.074807
This article has not been copyedited and formatted. The final version may differ from this version.

Interrelationships between Infliximab and rhTNF-α in Plasma using Minimal Physiologically-Based Pharmacokinetic (mPBPK) Models

Xi Chen, Debra C DuBois, Richard R Almon, William J Jusko

Department of Pharmaceutical Sciences, School of Pharmacy and Pharmaceutical Sciences, State University of New York at Buffalo, Buffalo, NY, 14214, USA (X.C., D.C.D, R.R.A, W.J.J.);

Department of Biological Sciences, State University of New York at Buffalo, Buffalo, NY, 14260, USA (D.C.D, R.R.A);

DMD Fast Forward. Published on April 14, 2017 as DOI: 10.1124/dmd.116.074807
This article has not been copyedited and formatted. The final version may differ from this version.

Running title: Pharmacokinetic Interactions of TNF-α and Infliximab

Corresponding author:

William J Jusko, Ph.D.

Department of Pharmaceutical Sciences

School of Pharmacy and Pharmaceutical Sciences

State University of New York at Buffalo

Buffalo, NY, 14214

Telephone: 716-645-2855

Fax: 716-829-6569

E-mail: wjjusko@buffalo.edu

Number of text pages: 21

Number of tables: 1

Number of figures: 6

Number of references: 30

Number of words:

Abstract: 191

Introduction: 668

Discussion: 1100

ABBREVIATIONS: IgG, immunoglobulin G; ISF, interstitial fluid; IV, intravenous; mPBPK, minimal physiologically-based pharmacokinetic model; PK, pharmacokinetics; RA, rheumatoid arthritis; rhTNF-α, recombinant tumor necrosis factor-alpha; TMDD, target-mediated drug disposition; TNF-α, tumor necrosis factor-alpha; SC, subcutaneous.

DMD Fast Forward. Published on April 14, 2017 as DOI: 10.1124/dmd.116.074807
This article has not been copyedited and formatted. The final version may differ from this version.

Abstract

The soluble cytokine TNF-α is an important target for many therapeutic proteins used in the treatment of rheumatoid arthritis (RA). Biologics targeting TNF-α exert their pharmacological effects through binding and neutralizing this cytokine and preventing it from binding to its cell surface receptors. The magnitude of their pharmacological effects directly corresponds to the extent and duration of free TNF-α suppression. However, endogenous TNF-α is of low abundance and therefore it is quite challenging to assess the free TNF-α suppression experimentally. Here we have applied an experimental approach to bypass this difficulty by giving rhTNF-α to rats by SC infusion. This boosted TNF-α concentration enabled quantification of TNF-α in plasma. Free rhTNF-α concentrations were measured after separation from the infliximab-rhTNF-α complex using Dynabeads Protein A. The interrelationship of infliximab and TNF-α was assessed with minimal physiologically-based pharmacokinetic (mPBPK) models for TNF-α and infliximab with a target-mediated drug disposition (TMDD) component. Knowledge of TNF-α PK allows reliable prediction of the free TNF-α suppression with either free or total TNF-α concentration profiles. The experimental and modeling approaches in the present study may aid in the development of next-generation TNF-α inhibitors with improved therapeutic effects.

Introduction

Pro-inflammatory soluble cytokines, including TNF-α, are key players in the pathogenesis of rheumatoid arthritis (RA). These cytokines, along with immune cells, form an inter-connected network. In inflammatory conditions, these cytokines exhibit elevated and sustained expression and their production is dysregulated (Buchan et al., 1988). TNF-α is at the apex of this network and fulfills its mission through binding to its cell surface receptors, activating downstream inflammatory response cascades, and promoting expression of other cytokines (Fong et al., 1989). Previous work showed that blocking TNF-α itself led to substantial inhibitory effects on the expression of other pro-inflammatory cytokines (Brennan et al., 1989) and reduced leucocyte trafficking into the joints (Taylor et al., 2000), and thus highlighted the importance of TNF-α as a therapeutic target for the treatment of RA (Monaco et al., 2015).

Anti-TNF-α therapy is now the standard of care for RA. The TNF-α antagonists, including infliximab, etanercept and adalimumab, alone or in combination with methotrexate, are quite efficacious in the treatment of RA (Upchurch and Kay, 2012). The great success of current anti-TNF-α biologics has triggered efforts in seeking new biological agents targeting TNF-α with improved features using advanced protein engineering techniques. Biologics targeting TNF-α exert their pharmacological effects through binding and neutralizing this cytokine and preventing it from binding to its cell surface receptors. The magnitude of their pharmacological effects directly corresponds to the extent and duration of free TNF-α suppression. Quantitative characterization of the mechanistic cascades that lead to TNF-α suppression by therapeutic proteins would help to better understand the exposure-response relationship, aid identification of desired pharmacokinetic (PK) and target-binding features for next generation anti-TNF-α biological agents.

TNF-α, as a soluble cytokine protein, exhibits rapid turnover with a plasma half-life in minutes. This feature leads to substantial accumulation of TNF-α in circulation when biologics bind to TNF-α as a carrier and increases its retention time in blood. In such cases, receptor occupancy (RO) obtained based on the PK of the biologic alone does not correlate with the duration of TNF-α suppression. The TMDD kinetics (Mager, 2006) characterizing the interaction between anti-TNF-α agents and their targets serve as an alternative to assess TNF-α suppression.

The second-generation minimal physiologically-based pharmacokinetic (mPBPK) models with implemented TMDD features proposed and assessed by Cao and Jusko (Cao et al., 2013; Cao and Jusko, 2014a) offer a suitable modeling platform to assess pharmacokinetics of monoclonal antibodies (mAbs) and other therapeutic proteins, as well as their interplay with antigenic targets either in plasma or in tissues. With essential components for mAb PK inherited from full PBPK models, the mPBPK model is structured in an anatomical manner with plasma, lymph and lumped tissue compartments. Para-vascular convection and lymph drainage are the dominant pathways for mAb movement from plasma to tissue sites and return to plasma. Tissue interstitial space is assumed to be the major extravascular distribution space. Of importance, TMDD features can be readily implemented in both plasma and tissues for assessment of the mAb interaction with antigenic targets. In addition, the physiological and anatomical layouts of the mPBPK model allow it to be feasibly overlaid with other physiologically-based pharmacokinetic (PBPK) models, and thus enables assessment of two or more protein compounds and their interactions. We have previously applied such models for the characterization of the suppression of IL-6 by an anti-IL-6 mAb in serum as well as in joint synovial fluid in collagen-induced arthritic (CIA) mice (Chen et al., 2016).

In the present study, the interaction of infliximab and TNF-α in rats was examined and mPBPK models were applied to quantitatively describe the time-course of TNF-α suppression by infliximab. To fully characterize the TMDD kinetics, measurements of both infliximab and TNF-α are required. However, the low abundance of endogenous TNF-α makes its measurement technically challenging (Manicourt et al., 1993; Gratacos et al., 1994). To overcome this problem, rhTNF-α was administered to the rats as an infusion, which boosted the baseline of TNF-α and enabled its quantification. Infliximab is a chimeric mAb and does not cross-react with rodent TNF-α and thus interference with endogenous rat TNF-α was avoided.

Materials and Methods

Test Articles. Infliximab (Janssen Biotech Inc, Horsham, PA) was first reconstituted with 10 mL of sterile water at 10 mg/mL, and further diluted with sterile saline when needed. The reconstituted infliximab was stored at 2-8˚C before use. Recombinant human TNF-α (rhTNF-α) obtained from R&D Systems (Minneapolis, MN, Catalog Number 210-TA-02M/CF) was reconstituted with sterile phosphate buffered saline (PBS) solution (pH 7.4) containing 0.1% bovine serum albumin (BSA) at 2 mg/mL. The reconstituted rhTNF-α was stored in aliquots at -80˚C before use.

Animals. Male Lewis rats (300 g) were purchased from Harlan (Indianapolis, IN). Animals were housed individually in the University Laboratory Animal Facility and acclimatized for 1 week with free access to food and water at constant environmental conditions (22˚C, 72% humidity, and 12-h light/12-h dark cycles). All animal study protocols followed the Principles of Laboratory Animal Care (Institute of Laboratory Animal Resources, 1996) and were approved by the University at Buffalo Institutional Animal Care and Use Committee.

Assays. Infliximab concentrations in plasma were measured using an anti-human IgG ELISA kit (Bethyl Laboratories, Montgomery, TX), as previously described (Lon et al., 2012). The lack of interference of TNF-α in infliximab measurements was confirmed by setting up *in vitro* plasma samples containing infliximab together with various concentrations of rhTNF-α. The concentrations of infliximab in the *in vitro* plasma samples were set to match the lower and higher end of infliximab PK profiles in the animal studies.

Plasma concentrations of rhTNF-α were assayed with the human TNF-α Quantikine HS ELISA kit (R&D Systems, Minneapolis, MN) following the instructions of the manufacturer. The standard curve was fitted to a four-parameter logistic model and ranged 0.5 – 32 pg/mL.

Between assay variability was tested with quality control (QC) samples (2 and 20 pg/mL) prepared by adding rhTNF-α to blank rat plasma, and was typically less than 15%. The cross-species reactivity was minimal with rat plasma.

Dynabeads Protein A (Life Technologies, Grand Island, NY) was used to remove infliximab and infliximab-bound TNF-α and thus obtain free rhTNF-α in the plasma samples. These magnetic beads have Protein A (a bacterial protein with strong binding affinity to IgG) covalently coupled to their surface. The capacity of Dynabeads Protein A (30 mg/mL) is approximately 8 μg human IgG per mg beads, and infliximab in both free and bound forms binds tightly in this matrix. Aliquots of the beads (100 μL) were transferred to 0.5 mL microfuge tubes and separation achieved using a magnetic rack. The buffer solution was removed, and then plasma samples of 50 μL were added into the tube and incubated for 10 min with gentle rotation at room temperature. After incubation the tube was placed on the magnet rack and the supernatant containing only free rhTNF-α was collected for quantification. Assay optimization and validation were performed by running a set of blank plasma samples containing infliximab (2 μg/mL)) with various volumes of Dynabeads Protein A and testing the obtained supernatants for residual infliximab.

Animal Study. The pharmacokinetics of infliximab in healthy Lewis rats (IV at 1 and 10 mg/kg) were previously examined in our lab. Lewis rats (n = 2) received an IV bolus dose of infliximab at 0.1 mg/kg and serial blood samples were collected at 0.5, 2, 5 and 10 h, and 1, 2, 4, 6 and 10 days from the saphenous vein under short-term anesthesia by inhalation of 3% isoflurane and at 14 days from the abdominal aorta by exsanguination upon sacrifice.

Another group of rats (n = 6) were used for assessing the suppression of rhTNF-α by infliximab. Animals received an IV bolus dose of infliximab (0.1 mg/kg). In addition SC

infusion of rhTNF-α at 117.4 μg/kg/day for 48 h began at the time of infliximab injection, using the Alzet micro-osmotic pumps (Model 1003D, infusion rate 1 μL/h, Durect Corporation, Cupertino, CA). The pumps were implanted into a skin pocket on the animals back under isoflurane anesthesia. The rats were monitored for allergic or toxic reactions and rectal temperatures were recorded periodically. Serial blood samples were collected at 2, 5, 7, 10, 13, 16, 20, 25 and 35 h from the saphenous vein under short-term anesthesia by inhalation of 3% isoflurane and at 40 and 48 h from the abdominal aorta by exsanguination upon sacrifice. Three animals were sampled for blood at each time point. Blood samples were immediately centrifuged at 2,000×*g*, 4ºC for 15 min. The plasma fraction was aliquoted and stored at -80ºC.

Mathematical Modeling. To quantitatively capture the interrelationship between infliximab and rhTNF-α in plasma, a step-wise modeling strategy was performed. The PK of infliximab and rhTNF-α were first characterized with mPBPK models, and then both mPBPK models were combined and TMDD kinetic features added in order to assess the suppression of rhTNF-α by infliximab. The PK-related parameters for infliximab estimated from the initial modeling step and for rhTNF-α obtained from our companion study (Chen et al, 2017) were fixed in the subsequent model fitting for assessment of the interaction of infliximab and rhTNF-α.

The PK of infliximab was captured with the second-generation mPBPK model. Mean concentration-time profiles of infliximab at 1 and 10 mg/kg and naïve-pooled concentration-time profiles of infliximab at 0.1 mg/kg in plasma were assessed. The model includes plasma, lymph, and two lumped tissue compartments connected in an anatomical manner, as shown in Figure 1 (Cao et al., 2013). Clearance of infliximab is assumed from the systemic circulation. The model is described as:

DMD Fast Forward. Published on April 14, 2017 as DOI: 10.1124/dmd.116.074807
This article has not been copyedited and formatted. The final version may differ from this version.

$$\frac{dC_{p_D}}{dt} = \frac{C_{lymph} \cdot L - C_{p_D} \cdot L_1 \cdot (1-\sigma_1) - C_{p_D} \cdot L_2 \cdot (1-\sigma_2) - C_{p_D} \cdot CL_{mAb}}{V_p}$$

$$C_{p\_D}(0) = \frac{Dose}{V_p} \qquad (1)$$

$$\frac{dC_{tight}}{dt} = \frac{C_{p_D} \cdot L_1 \cdot (1-\sigma_1) - L_1 \cdot (1-\sigma_L) \cdot C_{tight}}{V_{tight}} \qquad C_{tight}(0) = 0 \qquad (2)$$

$$\frac{dC_{leaky}}{dt} = \frac{C_{p_D} \cdot L_2 \cdot (1-\sigma_2) - L_2 \cdot (1-\sigma_L) \cdot C_{leaky}}{V_{leaky}} \qquad C_{leaky}(0) = 0 \qquad (3)$$

$$\frac{dC_{lymph}}{dt} = \frac{L_1 \cdot (1-\sigma_L) \cdot C_{tight} + L_2 \cdot (1-\sigma_L) \cdot C_{leaky} - C_{lymph} \cdot L}{V_{lymph}} \qquad C_{lymph}(0) = 0 \qquad (4)$$

where C_{p_D} is the plasma concentration of infliximab in V_p (plasma volume), C_{tight} and C_{leaky} are *ISF* concentrations of infliximab in two types of lumped tissues categorized by the leakiness of vasculature, V_{tight} (0.65 • *ISF* • K_p, where K_p is the available fraction of ISF for antibody distribution) and V_{leaky} (0.35 • *ISF* • K_p) are *ISF* volumes of the two lumped tissues, V_{lymph} is the lymph volume, which equals blood volume, the L is the total lymph flow rate and L_1 and L_2 account for 1/3 and 2/3 of the total lymph flow, the σ_1 and σ_2 are vascular reflection coefficients for leaky and tight tissues, the σ_L is the lymphatic capillary reflection coefficients and is assumed to be 0.2, and CL_{mAb} is the linear clearance of infliximab.

The pharmacokinetics of rhTNF-α was previously described (Chen et al, 2017) with an extended first-generation mPBPK model and a semi-mechanistic model for SC absorption. The model structure (Figure 2) as well as parameter values that were estimated were then used as follows:

The SC absorption kinetics are:

$$\frac{dA_{dd}}{dt} = k_{inf} - \left(k_{aO} + k_{aL} + \frac{K_{max}}{KD_{50} + A_{dd}}\right) \cdot A_{dd} \qquad A_{dd}(0) = 0 \qquad (5)$$

DMD Fast Forward. Published on April 14, 2017 as DOI: 10.1124/dmd.116.074807
This article has not been copyedited and formatted. The final version may differ from this version.

$$\frac{dA_{OT1}}{dt} = k_{aO} \cdot (A_{dd} - A_{OT1}) \qquad A_{OT1}(0) = 0 \qquad (6)$$

$$\frac{dA_{OT2}}{dt} = k_{aO} \cdot (A_{OT1} - A_{OT2}) \qquad A_{OT2}(0) = 0 \qquad (7)$$

$$\frac{dA_{Lym}}{dt} = k_{aL} \cdot A_{dd} - L_a \cdot \frac{A_{Lym}}{V_{Lym}} \qquad A_{Lym}(0) = 0 \qquad (8)$$

where A_{dd}, A_{Lym}, A_{OT1} and A_{OT2} are the amounts of rhTNF-α at the SC injection site, lymph and two transit compartments (*OT1* and *OT2*), V_{Lym} is the lymph volume and equals blood volume, L_a is the lymph flow rate measured by thoracic duct cannulation (0.6 mL/h (Kojima et al., 1988)), k_{aL} and k_{aO} are absorption rate constants for rhTNF-α for lymph uptake and other routes, K_{max} and KD_{50} represent the saturable pre-systemic degradation at the SC injection site, and k_{inf} is the SC infusion rate.

The amount of rhTNF-α entering the systemic circulation (*Input*) is:

$$Input = L_a \cdot \frac{A_{Lym}}{V_{Lym}} + k_{aO} \cdot A_{OT2} \qquad (9)$$

Plasma pharmacokinetics of rhTNF-α are:

$$\frac{dC_{p\_T}}{dt} = \frac{Input}{V_p} - \frac{\left((f_{d1} + f_{d2}) \cdot (Q_{CO} - Q_k) + f_{dk} \cdot Q_k\right) \cdot C_{p\_T}}{V_p} + \frac{f_{d1} \cdot (Q_{CO} - Q_k) \cdot C_1}{V_p} + \frac{f_{d2} \cdot (Q_{CO} - Q_k) \cdot C_2}{V_p} + \frac{f_{dr} \cdot Q_k \cdot C_k}{V_p} - \frac{\frac{C_{p\_T} \cdot V_{max}}{C_{p\_T} + K_m}}{V_p} \qquad C_{p\_T}(0) = 0 \qquad (10)$$

$$\frac{dC_1}{dt} = \frac{f_{d1} \cdot (Q_{CO} - Q_k) \cdot \left(C_{p\_T} - \frac{C_1}{K_p}\right)}{V_1} \qquad C_1(0) = 0 \qquad (11)$$

$$\frac{dC_2}{dt} = \frac{f_{d2} \cdot (Q_{CO} - Q_k) \cdot \left(C_{p\_T} - \frac{C_2}{K_p}\right)}{V_2} \qquad C_2(0) = 0 \qquad (12)$$

DMD Fast Forward. Published on April 14, 2017 as DOI: 10.1124/dmd.116.074807
This article has not been copyedited and formatted. The final version may differ from this version.

$$\frac{dC_k}{dt} = \frac{f_{dk} \cdot Q_k \cdot \left(C_{p\_T} - \frac{C_k}{K_p}\right) - GFR \cdot GSC \cdot \frac{C_k}{K_p}}{V_k} \qquad C_k(0) = 0 \qquad (13)$$

where C_{p_T}, C_1, C_2 and C_k are concentrations of rhTNF-α in plasma (V_p), two tissue interstitial fluid (*ISF)* compartments (V_1 and V_2) and kidney *ISF* (V_k), Q_{CO} is cardiac plasma output, Q_k is the kidney plasma flow, f_{d1} and f_{d2} are the fractions of Q_{CO} for V_1 and V_2, f_{dk} is the fraction of Q_k for V_k, K_p is the tissue partition coefficient, *GFR* is the glomerular filtration rate, *GSC* is the glomerular sieving coefficient, and V_{max} and K_m terms account for the nonlinear elimination.

In the last step, the second- and first-generation mPBPK models were overlaid and the TMDD component was included in the plasma (Figure 3). The model includes infliximab plasma PK (Section A), rhTNF-α plasma PK (Section B), rhTNF-α SC absorption kinetics (Section C) and the interrelationship between infliximab and rhTNF-α (Section D). All PK-related parameters of infliximab and rhTNF-α were fixed. Plasma concentration-time profiles of total infliximab and free rhTNF-α were applied for simultaneous model fitting. Together with Eq. 5 – 9, the model is:

$$\frac{dC_{p\_D}}{dt} = \frac{C_{lymph} \cdot L - C_{p\_D} \cdot L_1 \cdot (1-\sigma_1) - C_{p\_D} \cdot L_2 \cdot (1-\sigma_2) - C_{p\_fD} \cdot CL_{mAb}}{V_p} - C_{p\_DT} \cdot k_{int}$$

$$C_{p\_D}(0) = \frac{Dose}{V_p} \qquad (14)$$

$$\frac{dC_{tight}}{dt} = \frac{C_{p\_D} \cdot L_1 \cdot (1-\sigma_1) - L_1 \cdot (1-\sigma_L) \cdot C_{tight}}{V_{tight}} \qquad C_{tight}(0) = 0 \qquad (15)$$

$$\frac{dC_{leaky}}{dt} = \frac{C_{p\_D} \cdot L_2 \cdot (1-\sigma_2) - L_2 \cdot (1-\sigma_L) \cdot C_{leaky}}{V_{leaky}} \qquad C_{leaky}(0) = 0 \qquad (16)$$

$$\frac{dC_{lymph}}{dt} = \frac{L_1 \cdot (1-\sigma_L) \cdot C_{tight} + L_2 \cdot (1-\sigma_L) \cdot C_{leaky} - C_{lymph} \cdot L}{V_{lymph}} \qquad C_{lymph}(0) = 0 \qquad (17)$$

DMD Fast Forward. Published on April 14, 2017 as DOI: 10.1124/dmd.116.074807
This article has not been copyedited and formatted. The final version may differ from this version.

$$\frac{dC_{p\_T}}{dt} = \frac{Input}{V_p} - \frac{\left((f_{d1} + f_{d2}) \cdot (Q_{CO} - Q_k) + f_{dk} \cdot Q_k\right) \cdot (C_{p\_T} - C_{p\_DT})}{V_p}$$

$$+ \frac{f_{d1} \cdot (Q_{CO} - Q_k) \cdot C_1}{V_p} + \frac{f_{d2} \cdot (Q_{CO} - Q_k) \cdot C_2}{V_p} + \frac{f_{dr} \cdot Q_k \cdot C_k}{V_p}$$

$$- \frac{\frac{(C_{p\_T} - C_{p\_DT}) \cdot V_{max}}{(C_{p\_T} - C_{p\_DT}) + K_m}}{V_p} - C_{p\_DT} \cdot k_{int} \qquad C_{p\_T}(0) = \frac{Dose}{V_p} \qquad (18)$$

$$\frac{dC_1}{dt} = \frac{f_{d1} \cdot (Q_{CO} - Q_k) \cdot \left((C_{p\_T} - C_{p\_DT}) - \frac{C_1}{K_p}\right)}{V_1} \qquad C_1(0) = 0 \qquad (19)$$

$$\frac{dC_2}{dt} = \frac{f_{d2} \cdot (Q_{CO} - Q_k) \cdot \left((C_{p\_T} - C_{p\_DT}) - \frac{C_2}{K_p}\right)}{V_2} \qquad C_2(0) = 0 \qquad (20)$$

$$\frac{dC_k}{dt} = \frac{f_{dk} \cdot Q_k \cdot \left((C_{p\_T} - C_{p\_DT}) - \frac{C_k}{K_p}\right) - GFR \cdot GSC \cdot \frac{C_k}{K_p}}{V_k} \qquad C_k(0) = 0 \qquad (21)$$

where C_{p_fD} is the free infliximab concentration in plasma, C_{p_DT} is the concentration of the infliximab-rhTNF-α complex, k_{int} is the elimination rate constant for infliximab-rhTNF-α complex, and other symbols are as previously defined.

The model assumes that the infliximab-rhTNF-α complex will distribute into tissues in the same manner as free infliximab, and returns to plasma from tissues as free infliximab. This assumption is based on the fact that infliximab is largely diluted in tissues and the complex will thus dissociate. Also, the proteases that are present in the *ISF* space are expected to be constantly degrading the rhTNF-α freed from the dissociation of the complex.

Long-term rhTNF-α infusion caused mild fever and inflammatory reactions in the animals, which led to increased plasma clearances of infliximab and the infliximab-rhTNF-α complex. Therefore, CL_{mAb} and k_{int} were described with sigmoid functions to account for acute changes over a short time:

DMD Fast Forward. Published on April 14, 2017 as DOI: 10.1124/dmd.116.074807
This article has not been copyedited and formatted. The final version may differ from this version.

$$CL_{mAb} = CL_{mAb\_ctrl} + \left(CL_{mAb\_dis} - CL_{mAb\_ctrl}\right) \cdot \frac{1}{1 + e^{-(t-T_{dis})*4}} \quad (22)$$

$$k_{int} = k_{int\_ctrl} + \left(k_{int\_dis} - k_{int\_ctrl}\right) \cdot \frac{1}{1 + e^{-(t-T_{dis})*4}} \quad (23)$$

where CL_{mAb_ctrl} and CL_{mAb_dis} are the infliximab plasma clearances in healthy and TNF-α induced inflammation conditions, k_{int_ctrl} and k_{int_dis} are the elimination rate constants for infliximab-rhTNF-α complex in healthy and TNF-α induced inflammation conditions, and T_{dis} represents the time when TNF-α induced inflammation occurs.

Assuming quasi-equilibrium conditions, C_{p_fD} is (Gibiansky et al., 2008):

$$C_{p\_fD} = \frac{\left(C_{p\_D} - K_{ss} - C_{p\_T}\right) + \sqrt{\left(C_{p\_D} - K_{ss} - C_{p\_T}\right)^2 + 4 \cdot C_{p\_D} \cdot K_{ss}}}{2} \quad (24)$$

The K_{ss} is the steady-state constant defined as:

$$K_{ss} = \frac{k_{int} + k_{off}}{k_{on}} \quad (25)$$

where the k_{on} and k_{off} refer to the binding association and dissociation rate constants of infliximab with rhTNF-α. The binding association rate constant (k_{on}) of infliximab was fixed to 10^5 $M^{-1} \cdot S^{-1}$ (Kim et al., 2007; Song et al., 2008). Then $Cp_{\_DT}$ can be described as:

$$C_{p\_DT} = C_{p\_T} \cdot \frac{C_{p\_fD}}{K_{ss} + C_{p\_fD}} \quad (26)$$

The free rhTNF-α concentration (C_{p_sfT}) measured in plasma samples is:

$$C_{p\_sfT} = C_{p\_T} \cdot \frac{K_D}{K_D + C_{p\_sfD}} \quad (27)$$

where K_D is the binding dissociation constant defined as:

$$K_D = \frac{k_{off}}{k_{on}} \quad (28)$$

DMD Fast Forward. Published on April 14, 2017 as DOI: 10.1124/dmd.116.074807
This article has not been copyedited and formatted. The final version may differ from this version.

The K_D instead of K_{ss} was applied for representation of free rhTNF-α concentration in plasma since plasma samples taken from animals are considered *in vitro* environments for the interaction of rhTNF-α and infliximab. The free concentration of infliximab is:

$$C_{p\_sfD} = \frac{\left(C_{p\_D} - K_D - C_{p\_T}\right) + \sqrt{\left(C_{p\_D} - K_D - C_{p\_T}\right)^2 + 4 \cdot C_{p\_D} \cdot K_D}}{2} \quad (29)$$

Data Analysis. Non-compartmental analysis (NCA) was performed with WinNonlin 6.1 (Phoenix, Pharsight Corporation, Palo Alto, CA). The areas under the concentration time curves (AUC) of infliximab in plasma were estimated by the trapezoidal rule. All model fittings were carried out with the ADAPT 5 computer program (Biomedical Simulations Resource, USC, Los Angeles, CA). Data were naïve pooled and fitted using the maximum likelihood algorithm. The variance model was defined as:

$$V_i = (\sigma_1 + \sigma_2 \cdot Y_i)^2$$

where V_i is the variance of the ith observation, σ_1 and σ_2 are additive and proportional variance model parameters, Y_i is the ith model prediction. The model performance was assessed by goodness-of-fit plots and the Akaike Information Criterion (AIC) values. Graphs were generated with the GraphPad Prism (GraphPad Software Inc, San Diego, CA).

DMD Fast Forward. Published on April 14, 2017 as DOI: 10.1124/dmd.116.074807
This article has not been copyedited and formatted. The final version may differ from this version.

Results

Analysis of Infliximab and rhTNF-α. Infliximab concentrations in plasma were assayed by ELISA. The concurrent presence of rhTNF-α, which binds to infliximab, could possibly interfere with infliximab measurements. To test this, blank plasma samples were prepared containing known concentrations of infliximab and rhTNF-α. The measured infliximab concentrations in the presence of rhTNF-α were consistent with the known infliximab concentrations present in the sample (data not shown), demonstrating that rhTNF-α does not affect the ELISA measurement of infliximab.

Free rhTNF-α in plasma was separated using Dynabeads Protein A. The Protein A coated on the magnetic beads binds to the Fc-region of human mAbs with high affinity, and therefore can be applied to remove infliximab in either free or rhTNF-α bound forms. Although the Dynabeads have a large capacity for removing human IgG (8 μg per mg beads), Protein A also binds to different forms of rodent IgGs that are present in the rat plasma samples with great abundance. Our assay optimization showed that a volume 100 μL of Dynabeads could efficiently remove over 95% of infliximab at a concentration of 2 μg/mL from 50 μL rat plasma.

Quantification of total rhTNF-α was attempted with acid/alkaline dissociation approaches (Salimi-Moosavi et al., 2010), but failed due to low recovery (<10%). TNF-α exists as homo-trimer in the biological fluid, but can dissociate into monomers at higher temperatures, acidic pH, and in the presence of nonionic detergents or surfactants (Smith and Baglioni, 1987; Corti et al., 1992; Poiesi et al., 1993). Also, the activity of TNF-α is sensitive to pH and is rapidly destroyed outside the pH range 5.5 – 10 (Haranaka et al., 1986). Acid/alkaline dissociation approaches require extreme pH conditions and lead to dissociation of the trimeric form of TNF-α or loss of activity, which likely explained the observed low recovery.

DMD Fast Forward. Published on April 14, 2017 as DOI: 10.1124/dmd.116.074807
This article has not been copyedited and formatted. The final version may differ from this version.

Plasma Pharmacokinetics of Infliximab. Non-compartmental analysis showed that infliximab exhibited linear pharmacokinetics in healthy rats across the dosage range of 0.1 – 10 mg/kg. The second-generation mPBPK model was applied to describe the plasma pharmacokinetics of infliximab. The model-fitted plasma concentrations of infliximab were overlaid with experimental measurements as shown in Figure 4. The parameter estimates are listed in Table 1, Section A. Overall, the model well-captured the plasma concentration-time profiles of infliximab at all doses. The estimated vascular reflection coefficients of tight and leaky tissue (σ_2 and σ_2) are 0.96 and 0.48, which correspond well to most therapeutic mAbs (Cao and Jusko, 2014b) and suggest modest tissue distribution. The plasma clearance of infliximab (CL_{mAb_ctrl}) is 0.069 mL/h, which translates to an elimination half-life around 3.8 days in rats.

Interrelationship between infliximab and rhTNF-α. To assess interactions between infliximab and rhTNF-α and examine free rhTNF-α suppression by the drug, infliximab and rhTNF-α were dosed concurrently by IV bolus and SC infusion, respectively. The SC infusion of rhTNF-α allowed continuous introduction of rhTNF-α into plasma, which resembles the production of endogenous TNF-α, but at much higher rates. Rats were monitored for signs of inflammatory reactions following rhTNF-α and exhibited mild fever at 5-10 h. Comparison of the plasma concentration-time profiles of infliximab at 0.1 mg/kg alone and with concurrent dosing of rhTNF-α as shown in Figure 5 showed a dramatic decline of infliximab concentrations after 5-10 h in rats receiving SC infusion of rhTNF-α. This indicates a rapid increase of plasma clearance of infliximab, which is likely due to the pathophysiological changes (inflammatory reactions or immunogenicity) following rhTNF-α. On the other hand, the plasma concentration-time profile of rhTNF-α exhibited multi-phasic characteristics **(**Figure 6**)**. The free rhTNF-α showed: 1) a rapid increase during the initial phase due to the SC infusion as well as the

substantial accumulation of total rhTNF-α upon binding to infliximab, 2) reached a 'steady-state' starting from 5-10 h, which is likely attributed to the rapid increase of infliximab-rhTNF-α complex clearance and the resulting faster elimination of total rhTNF-α, and 3) rapidly increased again at ~16 h eventually reaching a new 'steady-state' since infliximab was almost all cleared from plasma.

The second- and first- generation mPBPK models for infliximab and rhTNF-α were joined and the TMDD component was implemented in the plasma in order to examine the interrelationship of the two compounds. The concurrent treatment with rhTNF-α led to rapid elimination of infliximab starting from 5-10 h, which could be possibly attributed to pathophysiological changes (inflammatory reaction and/or immunogenicity) induced by rhTNF-α SC infusion. The model accounted for the change in clearance of infliximab as well as formation of a binding complex as reflected in their sigmoidal functions. The tissue distribution of infliximab was also likely altered corresponding to the pathophysiological changes. However, since changes in infliximab PK occurred several hours post-dosing, it is challenging to identify a change in tissue distribution from the PK profile, as the initial phase of the profile was compromised. Therefore, we assumed that tissue distribution of infliximab remains constant. The model also assumed no change on rhTNF-α PK, as suggested by previous reports that high dose rhTNF-α infusions show stationary PK (Greischel and Zahn, 1989).

The model-fitted concentration-time profiles of infliximab and rhTNF-α were overlaid with the experimental measurements. In general, the model well-captured the infliximab plasma concentration profile as well as the trend of the free rhTNF-α concentration curve, but showed over-estimation of free rhTNF-α at the early time points. Since the change in clearances of infliximab and its binding complex occurred quite early, data are rather limited at the initial

DMD Fast Forward. Published on April 14, 2017 as DOI: 10.1124/dmd.116.074807
This article has not been copyedited and formatted. The final version may differ from this version.

phase of the PK profiles for precise characterization of the binding and disposition of infliximab before the change of clearances happened. The parameter estimates are listed in Table 1. The estimated time when rhTNF-α-induced pathophysiological changes occurred (T_{dis}) is 7.5 h, corresponding with the time window when fever was observed. The plasma clearance of infliximab after T_{dis} (CL_{mAb_dis}) is 3.46 mL/h, which is a 50-fold increase in comparison with that (CL_{mAb_ctrl}) before T_{dis}. On the other hand, the elimination rate constants of infliximab-rhTNF-α complex (k_{int}) before and after T_{dis} are 0.020 and 9.3 h^{-1} (k_{int_ctrl} and k_{int_dis}), which translate to the plasma clearances of 0.18 and 84 mL/h and suggest an increase by 500-fold. The clearance of the complex in healthy conditions resembles the clearance of infliximab (0.18 versus 0.07 mL/h), whereas in the case of rhTNF-α-induced changes, the clearance of the complex is closer to the clearance of rhTNF-α (84 versus 100 mL/h). This explains the accumulation of total rhTNF-α and the rapid rise of free rhTNF-α at the beginning, but more sustained rhTNF-α suppression at later times when bound rhTNF-α was also quickly eliminated. The estimated K_D value is 0.43 nM, which well agrees with literature reported affinity measurements for infliximab (Kim et al., 2007; Song et al., 2008).

Discussion

Soluble pro-inflammatory cytokines, including TNF-α, IL-1 and IL-6, are targets of many therapeutic proteins for the treatment of RA. The magnitude of the pharmacological response of therapeutic proteins directly correlates with free cytokine suppression. The soluble cytokines commonly exhibit rapid turnover rates and short plasma half-lives (in minutes). Therapeutic proteins targeting soluble cytokines lead to free cytokine suppression, but also serve as carriers, extending their plasma retention and causing substantial accumulation of total cytokines. In such cases, the duration and extent of free cytokine suppression does not correspond with the receptor occupancy (RO), but requires quantitative understanding of the interplay of cytokines with therapeutic proteins using PK/PD modeling approaches.

The interaction between cytokines and therapeutic proteins can be quantitatively characterized with PK/PD modeling when PK measurements of both the protein drugs and the cytokine targets are available (Wang et al., 2014; Chen et al., 2016). However, measurement of TNF-α is extremely challenging. Firstly, endogenous TNF-α is present at low abundance (Manicourt et al., 1993; Gratacos et al., 1994) and binding to infliximab will further lead to the lowering of the free rhTNF-α concentrations. This causes difficulties in TNF-α quantification with most commercially available assay kits that do not meet the high sensitivity requirements. Our study provides a means to bypass this difficulty by giving the animals rhTNF-α through SC infusion. This boosted TNF-α concentration enables quantification of TNF-α in plasma. More importantly, doses of rhTNF-α through systemic infusion can be adjusted to resemble the differences of TNF-α exposure in plasma and tissue sites. Assessing the tissue distribution and suppression of TNF-α by therapeutic proteins at the site of action is usually technically more demanding and PK measurements at the tissue sites are subject to large variabilities. By

providing an infusion of rhTNF-α, it is possible to examine the suppression of TNF-α in blood. In addition, infliximab has minimal binding affinity to rat TNF-α and thus there will be low interference of rat endogenous TNF-α with infliximab binding. Secondly, the measurements of total and free TNF-α are fairly difficult, especially when specific capture and detection antibodies for free and total TNF-α are not available. Therefore, pre-treatments to dissociate bound TNF-α and/or separate free TNF-α are required prior to the bioanalytical assays. The dissociation methods are dependent on the relative denaturation and stability of therapeutic proteins and the ligand (Salimi-Moosavi et al., 2010). The TNF-α is more sensitive to pH, temperature, and surfactants compared to infliximab (Smith and Baglioni, 1987; Corti et al., 1992; Poiesi et al., 1993), and thus acid/alkaline treatments produce substantial loss of TNF-α and yield low recoveries. Several approaches are available for free ligand separation, including molecular sieving, solid phase extraction, and affinity separations with Protein A/G resin columns (Lee et al., 2011; Wang et al., 2014). All of these methods cause sample dilution, which leads to the shift of the binding equilibrium and will bias the measurement of free ligand (Lee et al., 2011). The present study applies the Dynabeads Protein A for separation of free TNF-α. This method is very rapid, requires small sample volumes and, most importantly, minimizes sample dilution, which makes it a useful approach for free ligand separation from mAb-bound complex.

The first- and second-generations of mPBPK models provide suitable modeling platforms for smaller proteins like cytokines and other therapeutic proteins. Here we have extended the applications of mPBPK modeling by combining the two mPBPK models to assess the interaction of the mAb and the cytokine. The mPBPK models are constructed in an anatomical manner and use physiological volume and flows for drug PK behaviors, thus enabling the assessment of the

interaction of two or more molecules with distinctive tissue distributions and elimination properties.

The step-wise modeling strategy was applied by characterizing the PK of infliximab and rhTNF-α independently and applying the information in the subsequent assessment of their interrelationship. The dataset includes PK of infliximab and rhTNF-α as well as their interaction, which are subject to different degrees of variability. Having PK-related parameters estimated first allowed characterization of infliximab binding and disposition with rhTNF-α (Chen et al., 2017).

Only free rhTNF-α concentration profiles were applied for model fitting and yielded reasonable estimates of the K_D values consistent with literature reports. In many cases, free and total ligand concentration profiles are not both available and it is questionable if reliable prediction could be obtained when only free or total ligand profiles are applied for model fitting. As discussed by Zheng et al. (Zheng et al., 2015), when only free or total ligand concentrations are available, knowledge of either free ligand turnover rate or the in vivo K_D value would allow better prediction of free ligand suppression. *A priori* knowledge of TNF-α PK is fairly important for the characterizing free TNF-α suppression by mAbs, especially since total TNF-α quantification is extremely challenging.

The SC infusion of rhTNF-α at a relatively high dose resulted in pathophysiological changes in the rats. Therefore to characterize the suppression of free TNF-α, the impact of these disturbances on the PK of infliximab and rhTNF-α need to be considered. A dramatic increase in infliximab and the binding complex clearances was observed. Our data do not reflect the suppression of endogenous TNF-α with infliximab, probably due to pathophysiological changes, and a lower dose might avoid this change. Despite this, the data are informative regarding the

impact of the relative clearance time scales of infliximab, TNF-α, and the formed complex on the pattern of free TNF-α suppression. When the complex clearance is close to the clearance of infliximab (before T_{dis}), free TNF-α rapidly returns to baseline with substantial accumulation of total TNF-α. This is likely to represent TNF-α suppression in plasma where TNF-α is rapidly cleared, while infliximab and complex are sustained for longer times. On the other hand, when the complex clearance is similar to the clearance of TNF-α (after T_{dis}), the duration that free TNF-α suppression is prolonged, which resembles the situation in tissues, where both TNF-α and complex are assumed to be eliminated by lymph drainage.

In conclusion, the present study provides an experimental approach to examine the interrelationship between anti-TNF-α therapeutic proteins and endogenous TNF-α of low abundance *in vivo*, by giving the animal an infusion of TNF-α that boosts the baseline of TNF-α. The PK of infliximab and TNF-α was assessed with the first- and second-generation mPBPK models for TNF-α and infliximab with a TMDD component. Knowledge of TNF-α PK allows reliable assessment of the free TNF-α suppression with either free or total TNF-α concentration profiles. In this manuscript, the first- and second-generation mPBPK models developed for rhTNF-α and infliximab were overlaid with a TMDD component in the plasma compartment to examine the interaction of TNF-α and infliximab. This modeling framework could serve for extrapolation purposes with other TNF-α antagonists with substitution of their binding parameters for the ligands along with the independent measurements or predictions of the PK of the mAb and the PK of the ligand. However, this remains to be directly examined and proven experimentally.

Authorship Contributions

Participated in research design: Chen, DuBois, Almon, Jusko

Conducted experiments: Chen, DuBois

Performed data analysis: Chen, Jusko

Wrote or contributed to the writing of the manuscript: Chen, DuBois, Almon, Jusko

References

Brennan FM, Chantry D, Jackson A, Maini R, and Feldmann M (1989) Inhibitory effect of TNF alpha antibodies on synovial cell interleukin-1 production in rheumatoid arthritis. *Lancet* **2:**244-247.

Buchan G, Barrett K, Turner M, Chantry D, Maini RN, and Feldmann M (1988) Interleukin-1 and tumour necrosis factor mRNA expression in rheumatoid arthritis: prolonged production of IL-1 alpha. *Clin Exp Immunol* **73:**449-455.

Cao Y, Balthasar JP, and Jusko WJ (2013) Second-generation minimal physiologically-based pharmacokinetic model for monoclonal antibodies. *J Pharmacokinet Pharmacodyn* **40:**597-607.

Cao Y and Jusko WJ (2014a) Incorporating target-mediated drug disposition in a minimal physiologically-based pharmacokinetic model for monoclonal antibodies. *J Pharmacokinet Pharmacodyn* **41:**375-387.

Cao Y and Jusko WJ (2014b) Survey of monoclonal antibody disposition in man utilizing a minimal physiologically-based pharmacokinetic model. *J Pharmacokinet Pharmacodyn* **41:**571-580.

Chen X, Jiang X, Jusko WJ, Zhou H, and Wang W (2016) Minimal physiologically-based pharmacokinetic (mPBPK) model for a monoclonal antibody against interleukin-6 in mice with collagen-induced arthritis. *J Pharmacokinet Pharmacodyn* **43:**291-304.

Chen X, DuBois DC, Almon RR, and Jusko WJ (2017) Characterization and interspecies scaling of rhTNF-a pharmacokinetics with minimal physiologically-based pharmacokinetic models, Submitted for publication.

Corti A, Fassina G, Marcucci F, Barbanti E, and Cassani G (1992) Oligomeric tumour necrosis factor alpha slowly converts into inactive forms at bioactive levels. *Biochem J* **284 (Pt 3):**905-910.

Davies B and Morris T (1993) Physiological parameters in laboratory animals and humans. *Pharm Res* **10:**1093-1095.

Fong Y, Tracey KJ, Moldawer LL, Hesse DG, Manogue KB, Kenney JS, Lee AT, Kuo GC, Allison AC, Lowry SF, and et al. (1989) Antibodies to cachectin/tumor necrosis factor reduce interleukin 1 beta and interleukin 6 appearance during lethal bacteremia. *J Exp Med* **170:**1627-1633.

Gibiansky L, Gibiansky E, Kakkar T, and Ma P (2008) Approximations of the target-mediated drug disposition model and identifiability of model parameters. *J Pharmacokinet Pharmacodyn* **35:**573-591.

Gratacos J, Collado A, Filella X, Sanmarti R, Canete J, Llena J, Molina R, Ballesta A, and Munoz-Gomez J (1994) Serum cytokines (IL-6, TNF-alpha, IL-1 beta and IFN-gamma) in ankylosing spondylitis: a close correlation between serum IL-6 and disease activity and severity. *Br J Rheumatol* **33:**927-931.

Greischel A and Zahn G (1989) Pharmacokinetics of recombinant human tumor necrosis factor alpha in rhesus monkeys after intravenous administration. *J Pharmacol Exp Ther* **251:**358-361.

Haranaka K, Carswell EA, Williamson BD, Prendergast JS, Satomi N, and Old LJ (1986) Purification, characterization, and antitumor activity of nonrecombinant mouse tumor necrosis factor. *Proceedings of the National Academy of Sciences of the United States of America* **83:**3949-3953.

Kim MS, Lee SH, Song MY, Yoo TH, Lee BK, and Kim YS (2007) Comparative analyses of complex formation and binding sites between human tumor necrosis factor-alpha and its three antagonists elucidate their different neutralizing mechanisms. *J Mol Biol* **374:**1374-1388.

Kojima K, Takahashi T, and Nakanishi Y (1988) Lymphatic transport of recombinant human tumor necrosis factor in rats. *J Pharmacobiodyn* **11:**700-706.

Lee JW, Kelley M, King LE, Yang J, Salimi-Moosavi H, Tang MT, Lu JF, Kamerud J, Ahene A, Myler H, and Rogers C (2011) Bioanalytical approaches to quantify "total" and "free" therapeutic antibodies and their targets: technical challenges and PK/PD applications over the course of drug development. *AAPS J* **13:**99-110.

Lon HK, Liu D, and Jusko WJ (2012) Pharmacokinetic/pharmacodynamic modeling in inflammation. *Crit Rev Biomed Eng* **40:**295-312.

Mager DE (2006) Target-mediated drug disposition and dynamics. *Biochem Pharmacol* **72:**1-10.

Manicourt DH, Triki R, Fukuda K, Devogelaer JP, Nagant de Deuxchaisnes C, and Thonar EJ (1993) Levels of circulating tumor necrosis factor alpha and interleukin-6 in patients with rheumatoid arthritis. Relationship to serum levels of hyaluronan and antigenic keratan sulfate. *Arthritis Rheum* **36:**490-499.

Monaco C, Nanchahal J, Taylor P, and Feldmann M (2015) Anti-TNF therapy: past, present and future. *Int Immunol* **27:**55-62.

Poiesi C, Albertini A, Ghielmi S, Cassani G, and Corti A (1993) Kinetic analysis of TNF-alpha oligomer-monomer transition by surface plasmon resonance and immunochemical methods. *Cytokine* **5:**539-545.

Salimi-Moosavi H, Lee J, Desilva B, and Doellgast G (2010) Novel approaches using alkaline or acid/guanidine treatment to eliminate therapeutic antibody interference in the measurement of total target ligand. *Journal of Pharmaceutical and Biomedical Analysis* **51:**1128-1133.

Shah DK and Betts AM (2012) Towards a platform PBPK model to characterize the plasma and tissue disposition of monoclonal antibodies in preclinical species and human. *J Pharmacokinet Pharmacodyn* **39:**67-86.

Smith RA and Baglioni C (1987) The active form of tumor necrosis factor is a trimer. *J Biol Chem* **262:**6951-6954.

Song MY, Park SK, Kim CS, Yoo TH, Kim B, Kim MS, Kim YS, Kwag WJ, Lee BK, and Baek K (2008) Characterization of a novel anti-human TNF-alpha murine monoclonal antibody with high binding affinity and neutralizing activity. *Exp Mol Med* **40:**35-42.

Taylor PC, Peters AM, Paleolog E, Chapman PT, Elliott MJ, McCloskey R, Feldmann M, and Maini RN (2000) Reduction of chemokine levels and leukocyte traffic to joints by tumor necrosis factor alpha blockade in patients with rheumatoid arthritis. *Arthritis Rheum* **43:**38-47.

Upchurch KS and Kay J (2012) Evolution of treatment for rheumatoid arthritis. *Rheumatology (Oxford)* **51 Suppl 6:**vi28-36.

Wang W, Wang X, Doddareddy R, Fink D, McIntosh T, Davis HM, and Zhou H (2014) Mechanistic pharmacokinetic/target engagement/pharmacodynamic (PK/TE/PD) modeling in deciphering interplay between a monoclonal antibody and its soluble target in cynomolgus monkeys. *AAPS J* **16:**129-139.

Zheng S, McIntosh T, and Wang W (2015) Utility of free and total target measurements as target engagement and efficacy biomarkers in biotherapeutic development--opportunities and challenges. *J Clin Pharmacol* **55 Suppl 3:**S75-84.

Footnotes

This work was supported by the National Institute of General Medical Sciences, National Institutes of Health [Grant GM24211] and by the UB Center for Protein Therapeutics.

DMD Fast Forward. Published on April 14, 2017 as DOI: 10.1124/dmd.116.074807
This article has not been copyedited and formatted. The final version may differ from this version.

Legends for figures

Figure 1. Second-generation mPBPK model for characterization of infliximab plasma pharmacokinetics. Symbols are defined in Table 1.

Figure 2. Extended first-generation mPBPK model for characterization of rhTNF-α plasma pharmacokinetics and SC absorption kinetics. Model includes the absorption site, lymph, plasma and two transit compartments (*OT1* and *OT2*) for the characterization of rhTNF-α SC absorption and plasma compartment (V_p), two types of tissue compartments (V_1 and V_2), and the kidney (V_k) for the characterization of rhTNF-α distribution and disposition. Symbols are defined in Table 1.

Figure 3. Conjoined mPBPK models for infliximab and rhTNF-α with TMDD features implemented to assess the interrelationship between infliximab and rhTNF-α. Overall model structure includes: plasma PK of infliximab in Section A, plasma PK and SC absorption kinetics of rhTNF-α in Sections B and C, and interrelationship between infliximab and rhTNF-α in Section D. Symbols are defined in Table 1.

Figure 4. Infliximab concentration versus time profiles in plasma following IV administration at 0.1, 1 and 10 mg/kg. Symbols are observed concentrations and lines depict model-fitted profiles.

Figure 5. Plasma concentration versus time profiles of infliximab in animals receiving infliximab alone and with concurrent rhTNF-α SC infusion. Symbols are the individual and lines are the model-fitted infliximab plasma concentrations.

Figure 6. Plasma concentration versus time profiles of infliximab and free rhTNF-α in animals receiving an IV bolus of infliximab and SC infusion of rhTNF-α. Symbols are observed concentrations and lines depict model-fitted concentration profiles.

DMD Fast Forward. Published on April 14, 2017 as DOI: 10.1124/dmd.116.074807
This article has not been copyedited and formatted. The final version may differ from this version.

Table 1. Summary of model parameters and estimates.

Parameter (units)	Definition	Estimate	CV%
Section A: Plasma PK of Infliximab[a]			
σ_1	Vascular reflection coefficient of tight tissue	0.9650	13.1
σ_2	Vascular reflection coefficient of leaky tissue	0.4806	24.0
CL_{mAb_ctrl} (mL/h)	Plasma clearance before T_{dis}	0.06934	14.3
CL_{mAb_dis}* (mL/h)	Plasma clearance after T_{dis}	3.463	4.79
Section B: Plasma PK of rhTNF-α[b]			
f_{d1}	Fraction of (Q_{CO}-Q_k) for V_1	0.6663	
f_{d2}	Fraction of (Q_{CO}-Q_k) for V_2	0.007463	
f_{dk}	Fraction of Q_k for V_k	0.8	
K_p	Partition coefficient	0.5172	
V_1 (mL)	ECF volume for tissue compartment 1	13.10	
V_{max} (ng/h)	Michaelis-Menten capacity constant	3152	
K_m (ng/mL)	Michaelis-Menten affinity constant	31.72	
GSC	Glomerular sieving coefficient	0.1031	
f_{d1}	Fraction of (Q_{CO}-Q_k) for V_1	0.6663	
Section C: SC absorption of rhTNF-α[b]			
ka_O (1/h)	First-order absorption rate constant via other routes	0.4114	
ka_L (1/h)	First-order absorption rate constant via lymph	0.0007969	
K_{max} (ng/h)	Maximum degradation capacity at dose depot	899.9	
KD_{50} (ng)	Dose amount causing 50% of K_{max}	137.0	
ka_O (1/h)	First-order absorption rate constant via other routes	0.4114	
Section D: Interaction between infliximab and rhTNF-α			
k_{int_ctrl} (1/h)	Elimination rate constant of the complex before T_{dis}	0.01979	6.70
k_{int_dis} (1/h)	Elimination rate constant of the complex after T_{dis}	9.300	14.8
T_{dis} (h)	Time when rhTNF-α induced changes occurred	7.474	2.92
K_D (nM)	Binding dissociation constant	0.4297	7.84
Physiological values for rats (280 g)[c]			
V_p (mL)	Plasma volume	9.06	
V_{ECF} (mL)	Tissue extracellular fluid (ECF) volume	48.72	
Q_{CO} (mL/h)	Cardiac plasma output flow	2945	
Q_k (mL/h)	Renal plasma flow	365	
V_k (mL)	Kidney ECF volume	0.361	
GFR (mL/h)	Glomerular filtration rate	78.6	
V_{lymph} (mL)	Lymph volume	16.47	
L (mL/h)	Lymph flow rate	1.86	

[a] Parameters related to PK of infliximab were estimated first and fixed for model assessment of infliximab and rhTNF-α interactions.
[b] Parameters related to PK of rhTNF-α obtained from previous studies fixed for model assessment of infliximab and rhTNF-α interactions.

[c] Literature sources: all parameter values except *GFR* were from (Shah and Betts, 2012) and *GFR* values are from (Davies and Morris, 1993).
[*] Parameter estimated during the model assessment of infliximab and rhTNF-α interactions.

DMD Fast Forward. Published on April 14, 2017 as DOI: 10.1124/dmd.116.074807
This article has not been copyedited and formatted. The final version may differ from this version.

Figure 1

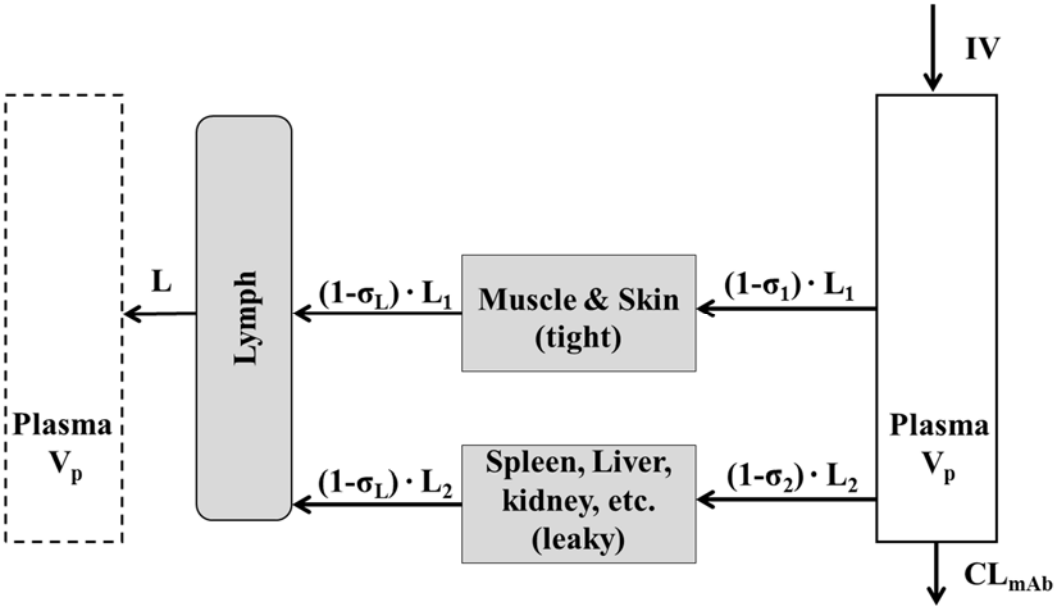

Figure 2

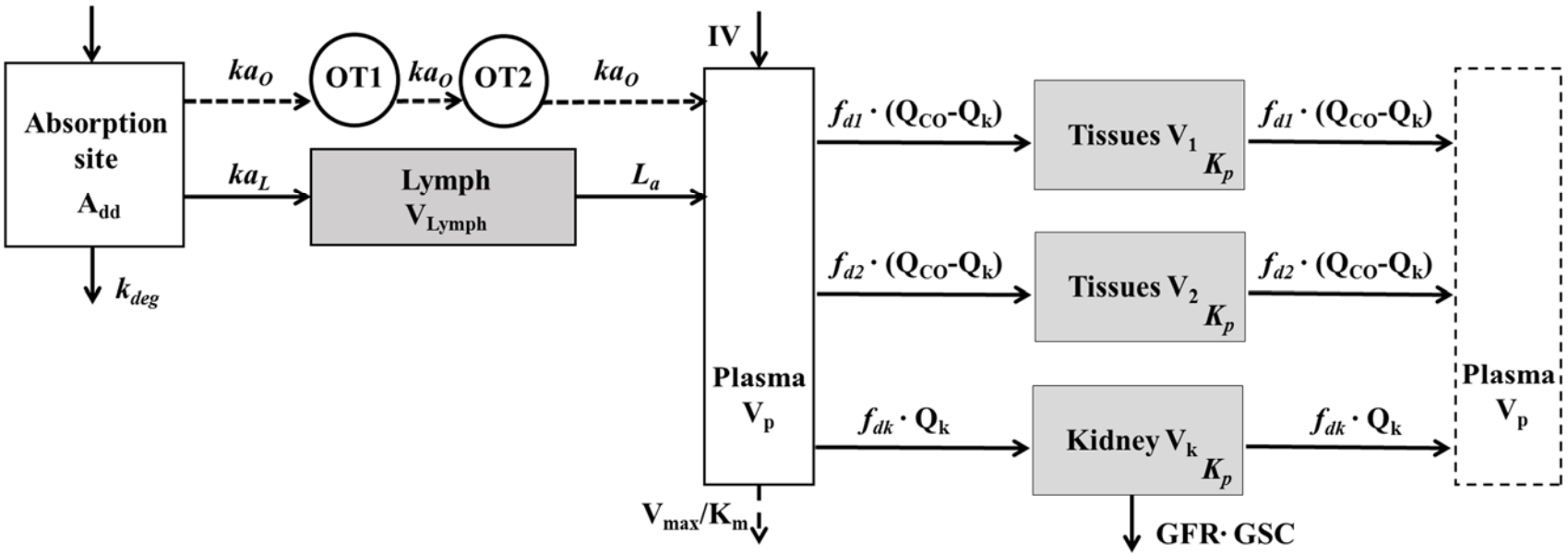

Figure 3

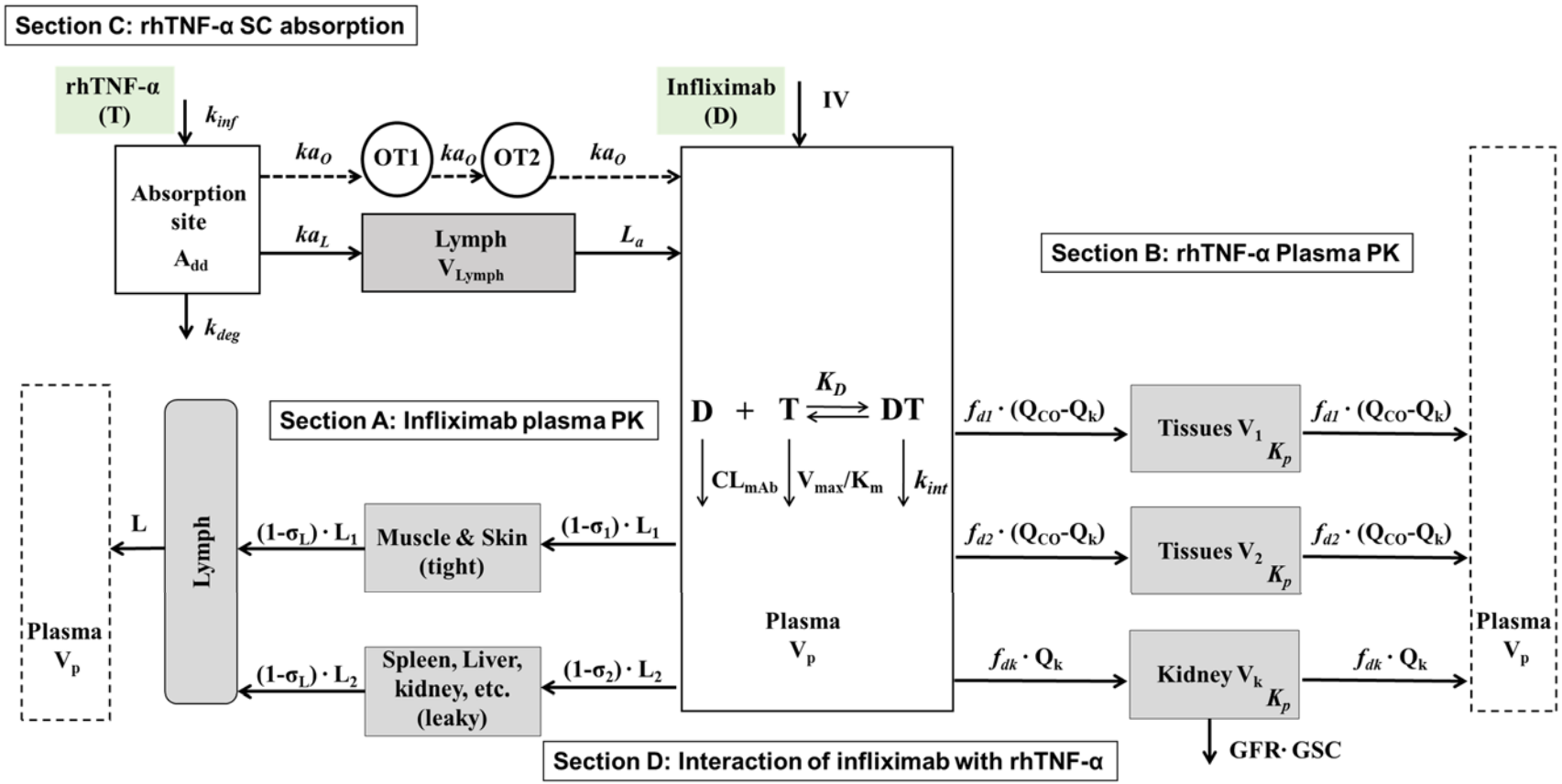

DMD Fast Forward. Published on April 14, 2017 as DOI: 10.1124/dmd.116.074807
This article has not been copyedited and formatted. The final version may differ from this version.

Figure 4

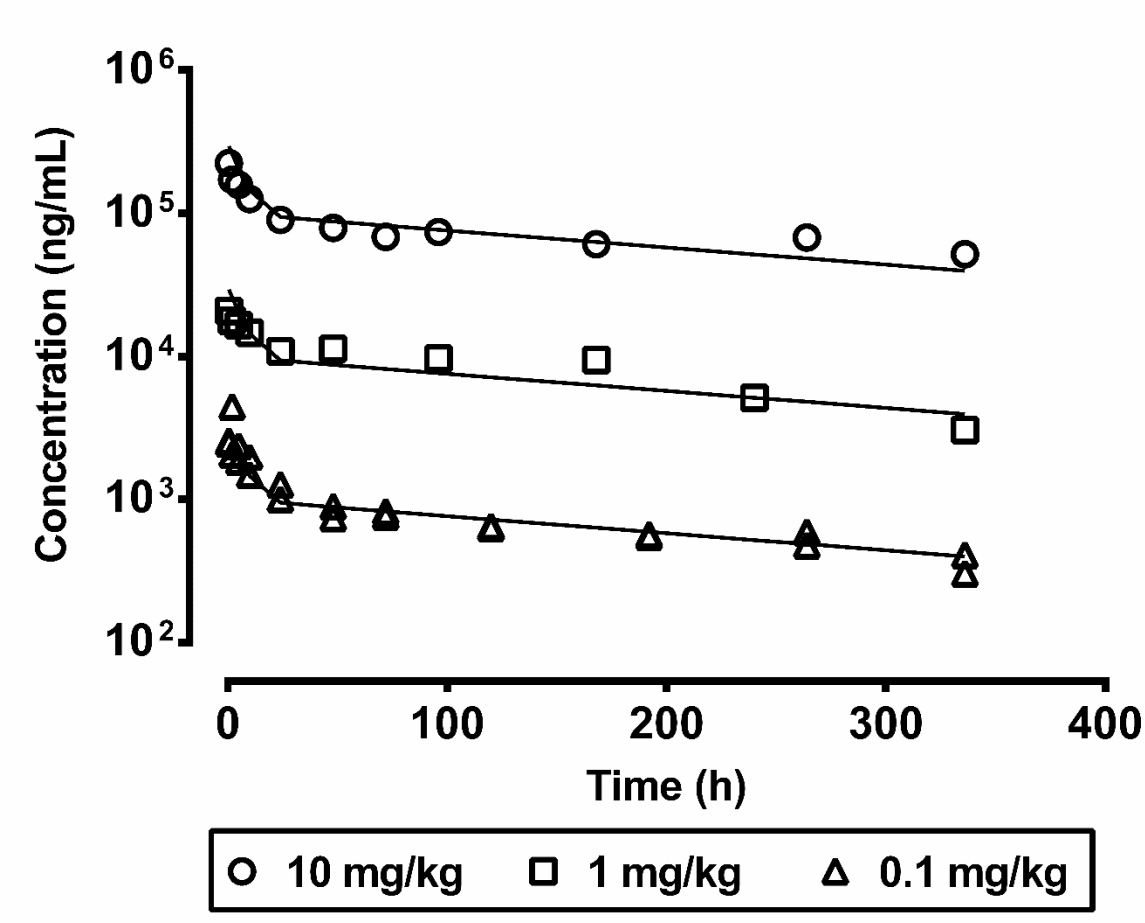

DMD Fast Forward. Published on April 14, 2017 as DOI: 10.1124/dmd.116.074807
This article has not been copyedited and formatted. The final version may differ from this version.

Figure 5

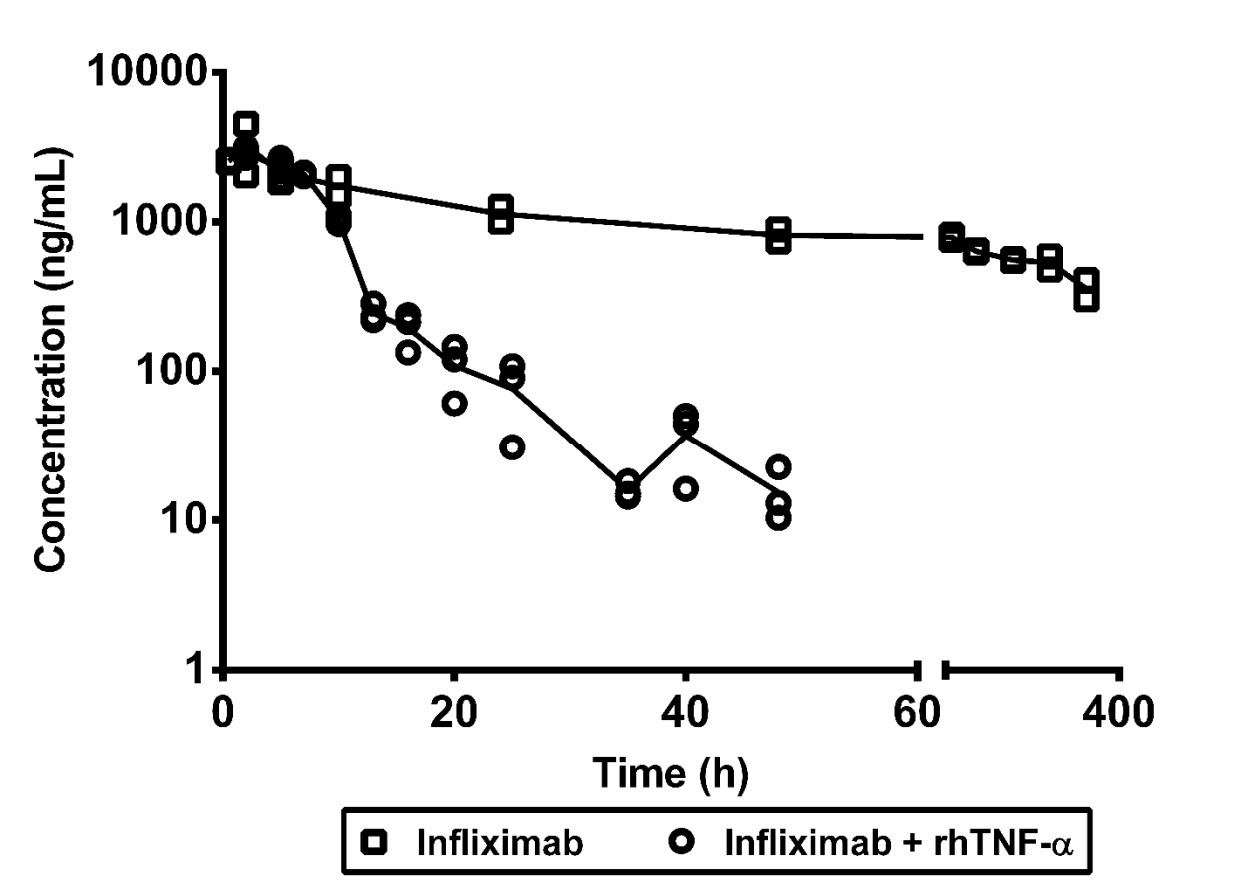

DMD Fast Forward. Published on April 14, 2017 as DOI: 10.1124/dmd.116.074807
This article has not been copyedited and formatted. The final version may differ from this version.

Figure 6